ACS OMEGA

http://pubs.acs.org/journal/acsodf

Article

Synthesis of Fatty Acid Methyl Ester from *Croton macrostachyus (Bisana)* Kernel Oil: Parameter Optimization, Engine Performance, and Emission Characteristics for *Croton macrostachyus* Kernel Oil Fatty Acid Methyl Ester Blend with Mineral Diesel Fuel

Zekarias Zeleke Zamba and Ali Shemsedin Reshad*

Cite This: *ACS Omega* 2022, 7, 20619−20633

Read Online

ACCESS | Metrics & More | Article Recommendations | Supporting Information

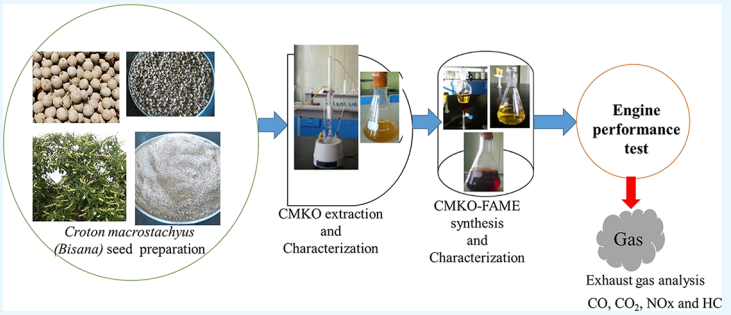

ABSTRACT: Utilization of agricultural waste such as nonedible seed oil for the synthesis of biodiesel via catalytic transesterification is one of the effective ways for the partial replacement of petroleum-based fuels in the area of renewable energy development and is beneficial to CO, CO_2, and unburned hydrocarbon (HC) emission reduction to the environment. In this regard, the current study investigates the synthesis of fatty acid methyl esters (FAMEs) from *Croton macrostachyus* kernel oil by considering parameter interaction and optimization to maximize the yield of fatty acid methyl esters (FAMEs). The response surface methodology−central composite design (RSM-CCD) was applied to optimize the *C. macrostachyus* fatty acid methyl ester (CMKO-FAME) synthesis process by varying the process parameters such as reaction time (1−2 h), molar ratio (6:1−12:1), and catalyst loading (1−2 wt %). The optimum conditions for the transesterification of *C. macrostachyus* kernel oil (CMKO) were found to be a methanol to oil ratio of 11.98:1, catalyst loading of 1.03 wt %, and reaction time of 2 h, resulting in the conversion of 95.03 wt % *C. macrostachyus* kernel oil into its mono FAMEs. The fuel properties of CMKO and its FAMEs were determined based on ASTM D6751 and EN 14214 standards. Further, the CMKO and its FAMEs were characterized using Fourier transform infrared (FT-IR), gas chromatography−mass spectrometry (GC−MS), and nuclear magnetic resonance spectroscopy (NMR). The fatty acid composition of CMKO was myristic acid (1.36%), palmitic acid (11.35%), stearic acid (5.11%), oleic acid (18.64%), gadoleic acid (0.34%), linoleic acid (49.084%), and linolenic acid (14.1%). The purity of the produced methyl esters was determined by ^{1}H NMR and found to be 95.52%, which was quite in good agreement with the experimentally observed yield of 95.39 wt %. The produced CMKO-FAME was blended with diesel fuel at various ratios (B5, B10, B15, and B20) to evaluate the engine performance and emission characteristics in a diesel engine. The engine brake thermal efficiency is lower, the brake-specific fuel consumption (BSFC) using CMKO-FAME blends is higher, and the temperature of exhaust gas emitted after combustion also increased as compared to diesel fuel. Similarly, using produced FAME blends, the emission emitted such as HC, NOx, and CO is reduced. However, the engine fueled with the produced FAME blends increased the level of CO_2 into the atmosphere when compared to diesel fuel. The performance and emission characteristics of diesel engine result show that the blend of CMKO-FAME and diesel can be used as a fuel in a diesel engine without any modification of the engine.

INTRODUCTION

The global energy consumption has been increasing multifold due to rapid population growth and economic development.[1−3] Currently, fossil fuels are the primary source that powers our modern world, and the reserves are likely to be depleted by 2052.[4] The production of alternative fuels from renewable sources has gained much interest from scientists,

Received: February 2, 2022
Accepted: May 27, 2022
Published: June 8, 2022

Table 1. Literature Summary on Various Feedstocks for Biodiesel Production at Various Reaction Conditions[d]

feedstock	parameter studied	catalyst	optimized condition	yield (%)	reference
DDSKO	MR, CL, and RT	NaOH	6.7:1, 0.79 wt %, and 60.5 °C	93.16	28
cotton seed oil	RV, CL, RT, and Rt	NaOH	20 vol %, 1 vol %, 60 °C, and 50 min	81%	29
neem seed oil		NaOH	100 min, 20%, 1%, and 60 °C	95%	
CMSO	MR, CL, and RT	KOH	6:1, 1 wt %, and 50 °C	96%	9
Jatropha−algae oil mixture	MR, CL, RT, and Rt	KOH	10:1, 0.3 wt %, 53 °C, 172 min	96%	30
waste cooking oil	MR, CL, RT, and Rt	CaO[c]	20:1, 5 wt %, 65 °C, and 4 h	96.74%[b]	31
Bauhinia variegata	MR, CL, RT, and Rt	Na_3PO_4	11:1, 2.96 wt %, 74 °C, and 45 min	95.1%[b]	32
waste cooking oil	MR, CL, RT, and Rt	TiO_2/GO	12:1, 1.5 wt %, 65 °C, and 3 h	98%[b]	33
castor seed[a]	MR, CL, RT, and Rt,	NaOH	200:1, 1.19 wt %, 30 °C, and 3 h	97%[b]	34

[a]In situ alkali-catalyzed transesterification process. [b]The transesterification product was analyzed by nuclear magnetic resonance spectroscopy (^{1}H and ^{13}C NMR) for conversion of oil into fatty acid alkyl esters (biodiesel). [c]Zn-doped CaO nanocatalyst. [d]RT: reaction temperature, Rt: reaction time, VR: volume ratio of methanol, MR: molar ratio of methanol to oil, CL: catalyst loading/concentration, DDSKO: desert date seed kernel oil, CMSO: *Croton macrostachyus* seed oil, TiO_2/GO: TiO_2 on reduced graphene oxide nanocomposite.

researchers, and industrialists in the field due to concerns on the depletion of fossil fuels and the impact of fossil fuel emissions on the environment.[5,6] More significantly, there is a critical need to ensure a sustainable supply of energy to fulfill the increasing energy demands, which is difficult with fossil fuels since these fuels are derived from nonrenewable sources. Biodiesel is one of the promising alternatives to mineral diesel fuel and is produced from renewable sources, nontoxic, nonflammable, portable, readily available, biodegradable, sustainable, eco-friendly, and free from sulfur and aromatic content.[3] However, more than 95% of biodiesel is produced from edible sources which has created concern about its impact on food supply. Hence, the concerns led to the development and enforcement of policies that emphasize the production of biofuels from agricultural byproduct and nonedible sources.[7] In response to this need, researchers are actively searching alternative nonedible feedstocks as well as microalgae and microalgae for the production of biodiesels.[8] Several researchers have proposed nonedible vegetable oils, animal fats, and waste cooking oil as feedstock for biodiesel production. The *Croton macrostachyus* seed is one of the promising agricultural byproducts (wastes). There are only few reports regarding the application of *C. macrostachyus* seed as a feedstock for biodiesel production, such as that by Aga *et al.* 2020.[9] All *C. macrostachyus* species grow fairly fast, have a wide weather tolerance, and grow over wide ranges of atmospheric conditions. *C. macrostachyus* grows at the mean annual rainfall between 1300 and 2500 mm and in the region between 1300 and 2500 m above sea level.[9] The mature seed of *C. macrostachyus* splits open with a sharp noise, and it contains from 45 to 58 wt % oil that is nonedible.[9]

Biodiesel is the fatty acid alkyl ester obtained by the transesterification reaction of vegetable oil triglycerides in the presence of a catalyst.[10] Reactants such as short-chain alcohol are widely used in the transesterification process.[11] The base-catalyzed transesterification process is the most commonly used method because it is carried out at a relatively low temperature (60 °C) with a faster rate as compared to the acid-catalyzed reaction.[12−14] The most common strong alkali catalysts being employed are sodium hydroxide (NaOH), potassium hydroxide (KOH), sodium methoxide (CH_3ONa), and potassium methoxide (CH_3OK).[15] Sodium hydroxide (NaOH) is preferred over potassium hydroxide (KOH) because it dissolves quickly in methanol to form methoxide. Several authors achieved different biodiesel yields via alkali-catalyzed transesterification (Table 1). Asmare and Gabbiye[16] achieved 94.5 wt % biodiesel yield at 1.22 wt % catalyst loading, 8.1:1 methanol to oil ratio, 59.89 °C reaction temperature, and constant reaction time and agitation speed of 2 h and 600 rpm, respectively. Similarly Meher *et al.*[17] achieved a 97 wt % biodiesel yield from Karanja oil at a rate of stirring of 180−600 rpm, temperature of 37−65 °C, catalyst loading of 0.25−1.5 wt %, and alcohol to oil molar ratio of 6:1−24:1 after 3 h reaction time. Basic type catalysts used for transesterification processes need a very high purity of raw materials with postreaction separation of the catalyst, by-product and product.[18]

For the conversion of vegetable oils into fatty acid alkyl esters, it is necessary to understand the effect of process variables on the fatty acid methyl ester/ethyl ester yield and fuel characteristics.[11] There are some very important reaction conditions to be given special attention to during the transesterification of vegetable oils to biodiesel, such as the alcohol to oil molar ratio, catalyst loading, and reaction time.[1] Therefore, the optimization of these parameters has an important effect on the mass production of FAME.[19] Biodiesel production process evaluation using one variable at a time does not show the interactive effect of process variables on the response function or biodiesel yield.[20] Artificial neural network (ANN) and response surface methodology (RSM) process modeling and optimization techniques can be used to predict the optimal process conditions for the transesterification reaction.[21,22] Both the RSM and ANN models predicted with comparably high accuracy the response optimization.[22,23] The ANN is basically a machine-based statistical approach that can be applied if precision is the major aim and more data are required for the optimization of the process response. Further, the technique does not show individual and interaction effects of the factors to the designed response. Moreover, the ANN technique is an efficient way of predicting and validating the results developed from any optimization technique.[21,24] The RSM model has been known as a powerful tool for optimization in several chemical, biological, and physical process analyses among many other applications.[25] RSM is a gathering of the statistical-based mathematical method and the most relevant multivariate technique for the process of transesterification of vegetable oil for modeling and optimization. The main advantage of the RSM method by performing the central composite design (CCD) is its capability to minimize the number of experimental runs needed to give adequate evidence for statistically acceptable results and assess the significance of the selected factor and the

https://doi.org/10.1021/acsomega.2c00682
ACS Omega 2022, 7, 20619−20633

individual and interaction effects on the designed response.[23,25,26] Therefore, RSM is a suitable statistical tool used to optimize the process parameters with a significantly reduced number of experiments for statistically relevant results.[27] The effects of individual parameters are also considered at the same time on the design response in RSM.

To provide a good balance of low temperature performance, low emissions, material compatibility, and the ability to act as a solvent, biodiesel has been used in diesel engines.[30,35] Significant research works have been reported with regard to the performance and emission characteristics of biodiesel derived from a variety of nonedible vegetable oils. Kumar *et al.*[30] reported on the production of biodiesel based on *Jatropha*−algae oil mixtures and the effect of biodiesel blends (B0, B5, B10, and B20 vol %) on the performance and emissions in a diesel engine coupled with an electricity generator fueled by the blends. The engine test results showed that the diesel fuel has the lowest BSFCs (340.2 g/kW) at full load and a higher BTE (23.11%) as compared to biodiesel blended fuel. In the same way, reduced HC and CO emission results with slightly increased NOx emission were found for B5, B10, and B20 vol % mixtures as compared to diesel fuel. Performance analysis on a diesel engine fueled with *Vachellia nilotica* seed oil methyl ester blends (5, 10, 15, and 20 vol % along with diesel fuel) was experimentally conducted by Sriharikota *et al.*[35] The engine tests were implemented by varying the brake power from 0 to 3.5 kW. The engine performance result revealed a lower thermal efficiency (7.34%) with an increased BSFC of 9.3% and exhaust gas temperature (EGT) of 14.28% for B20 as compared to mineral diesel fuel (0 vol %). Similarly, 20 vol % blending reduced the emission of HC and CO by 19.14 and 22.2%, respectively. Dhar and Agarwal[36] reported the maximum torque for 10 and 20% of Karanja oil methyl ester (KOME) blends that were higher than mineral diesel. Similarly, Raheman and Ghadge[37] found a comparable performance of Mahua (*Madhuca indica*) oil biodiesel and its blends with diesel. Khiari *et al.*[38] reported a 3% increase in thermal efficiency for *Pistacia lentiscus* biodiesel blends (with ratios of 5, 30, and 50 v/v %) at full engine load and 1500 rpm condition, which gave a satisfactory result in a diesel engine.[39] But Puhan *et al.*[40] noted a slight decrease in brake thermal efficiency (BTE) with linseed biodiesel compared to diesel fuel. Utlu and Kocak[41] reported that the brake specific fuel consumption (BSFC) was 14.34% higher than that of diesel fuel; this is due to the low heating value and the higher density of waste frying oil methyl ester. To the best of our knowledge, an analysis of the engine performance and emission characteristics of *C. macrostachyus* kernel oil fatty acid methyl ester blends with mineral diesel fuel has not been reported. Hence, the aim of the present study was to investigate the engine performance and emission characteristics of novel CMKO-FAME obtained at optimized conditions of the transesterification reaction blended with diesel fuel. Further, the present study was focused on the optimization of parameters such as the reaction time, molar ratio, and NaOH catalyst loading using the RSM-CCD method for the synthesis of *C. macrostachyus* kernel oil fatty acid methyl ester (CMKO-FAME). The obtained product was characterized for physicochemical values and its fatty acid composition to measure its suitability for engine performance and emission characteristics.

MATERIALS AND METHODS

Materials. The *C. macrostachyus* seed was collected from Loma Woreda, Ethiopia. The chemicals such as *n*-hexane (98%), ethanol (97%), sodium hydroxide (98%), potassium hydroxide (98%), anhydrous sodium thiosulfate (Na_2SO_4), Wij's solution, phosphoric acid, hydrochloric acid, diethyl ether, and methanol (98%) were purchased from Merck (Addis Ababa, Ethiopia, local supplier). All other reagents used in this study were purchased from Sigma-Aldrich (local supplier).

Methods. *C. macrostachyus Seed Pretreatment.* The *C. macrostachyus* seed was sun-dried for 7 days and decorticated manually to separate the seed shell from the kernel. After decortication, the outer shell of the seed was removed, and the kernels present inside the shell were separated and made into a powder with a particle size between 1 and 2 mm using a coffee grinder machine. Then the grounded *C. macrostachyus* kernel (CMK) was kept in a plastic bag until further use for the oil extraction process.

Extraction of CMK Oil. The CMKO was extracted as per the method described by Ilham and Saka.[42] One hundred grams of the powdered kernel of *C. macrostachyus* was put in a thimble of Soxhlet, and a flask containing 600 mL of *n*-hexane was stationed and placed in a condenser at the top of the Soxhlet chamber. The whole setup was heated up in a heating mantle at boiling temperature of the solvent (~65 °C) for 5 h. Then, the solvent was removed using rotary evaporators under a vacuum. The *C. macrostachyus* kernel oil was collected in the flask, and the yield was calculated according to eq 1 and pretreated before being used for the transesterification reaction:

$$Y_{\mathrm{CMKO}}(\mathrm{wt}\ \%) = \frac{M_{\mathrm{o}}}{M_{\mathrm{SK}}} \times 100 \tag{1}$$

where Y_{CMKO} is the yield of oil (wt %), M_{o} is the mass of oil extracted, and M_{SK} is initial mass of the seed kernel sample.

Transesterification of CMKO. The extracted oil was subjected to degumming with 1.5 wt % phosphoric acid (H_3PO_4) to remove the phospholipids and used for further reaction. The transesterification reaction was conducted in a 500 mL three-neck round-bottom flask (eq 2).

$$\text{1 mol of triglycerides of CMKO} + \text{3 mol of methanol} \Leftrightarrow \text{3 mol of CMKOME} + \text{1 mol of glycerol} \tag{2}$$

The parameters such as molar ratio (6:1 to 12:1 molar), catalyst loading (1 to 2 wt %), and reaction time (1 to 2 h) were considered for parameter optimization using RSM-CCD. For each experiment, initially, the oil sample was fed into the three-neck round-bottom flask and preheated at 70 °C for 0.5 h. And then the prepared sodium hydroxide and methanol solution was added to the preheated oil, and the mixture was agitated at 500 rpm and at 65 °C. At the completion of the transesterification process, the mixture underwent gravity settling in a separating funnel for 24 h to separate the glycerol and the *C. macrostachyus* kernel oil fatty acid methyl ester (CMKO-FAME) phase. The top phase containing the esters was collected and washed with hot distilled water (~50 °C) to remove residual impurities if any. Methanol and water were removed using a rotary evaporator at 70 °C under a vacuum. Finally, the CMKO-FAME yield (wt %) was calculated by relating the weight of CMKO and weight of CMKO-FAME

https://doi.org/10.1021/acsomega.2c00682
ACS Omega 2022, 7, 20619−20633

obtained using eq 3. Further, the CMKO-FAME properties such as density, viscosity, acid value, calorific value, saponification value, iodine value, flash point, and cetane number were determined and compared with ASTM D6751 and EN 14214 specification standards.[16]

$$Y(\text{wt \%}) = \frac{\text{amount of FAME obtained}}{\text{amount of oil sample used}} \times 100 \quad (3)$$

where Y is the yield of FAME (wt %).

Design of Experiment (DoE) for the Experimental Matrix. The response surface methodology (RSM) is a powerful technique to find the interaction effect of factors and optimize conditions when a number of factors are involved in the process and the response is affected by them.[2,28] The central composite design (CCD) is the most popular RSM design that fits an empirical polynomial model based on fractional factorial, axial, and center points. The technique also considers the interaction effect of the factors below the lower limit and above the upper limit of the factors. The experimental design matrix for RSM-CCD with three levels and three factors is $2^3 + 2 \times 3 + 6$. Hence, 20 experimental combinations were suggested by the experimental matrix. The average values of triplicates for each experimental results obtained from 20 experimental runs were analyzed statistically for CMKO-FAME production. Based on the experimental results, the quadratic polynomial equation (eq 4 in general form) was suggested by the DoE. To correlate the response (i.e., CMKO-FAME yield) with the independent process variables such as molar ratio (mole of methanol to oil ratio), catalyst loading (wt %), and reaction time (h), the suggested model equation was used. The quality of the model was investigated using multiple regressions (R^2), test of significance, and ANOVA. Further, numerical optimization was used to search the optimum condition for the synthesis of CMKO-FAME.

$$Y = \beta_o + \sum_{i=1}^{k} \beta_i X_i + \sum_{i=1}^{k} \beta_{ii} X^2{}_i + \sum_{j=1, j\neq i}^{k} \beta_{ij} X_i X_j + \xi \quad (4)$$

where Y is the response (CMKO-FAME yield), X_i and X_j are ith and jth independent process variables, β_o is a constant coefficient, β_i is the first-order model coefficient, β_{ij} is the linear model coefficient for the interaction between factors i and j, β_{ii} is the coefficient of quadratic effect of parameters, and ε is model random error.

Characterization of *C. macrostachyus* Kernel Oil, *C. macrostachyus* Kernel Oil FAME, and Its Blend with Diesel Fuel. *Physico-chemical Characterization.* Physico-chemical properties such as the density, viscosity, acid value, free fatty acid, saponification value, flash point, and iodine value were determined as per American Society for Testing and Materials (ASTM) methods. The calorific value[43] and cetane number[4] of the samples were determined using eqs 5 and 6, respectively.

$$\text{HHV (MJ/kg)} = 49.43 - [0.041\text{SV} + 0.015\text{IV}] \quad (5)$$

$$\text{CN} = 46.3 + \frac{54.58}{\text{SV}} - 0.225\text{IV} \quad (6)$$

where CN is the cetane number, SV is the saponification value, and IV is the iodine value of FAME.

Compositional Analysis. CMK, CMKO, and CMKO-FAME samples were analyzed using attenuated total reflectance Fourier transform infrared (FT-IR) (Shimadzu, Japan) and gas chromatography−mass spectrometry (GC−MS OP 5000 series, Shimadzu Japan, 2010) to identify the functional groups and chemical compositions, respectively.

FT-IR Analysis. Initially, the blank accessory ATR crystal was used to obtain the background FT-IR spectrum. Approximately 20 mg of the samples was placed in the sampling accessory ATR crystal. The entire spectrum was recorded with a range of 4000−500 cm^{-1} wave number with 4 cm^{-1} resolution and scan speed of 20 scans.

GC−MS Analysis. A capillary column of 60 m length, 0.25 mm internal diameter, and 0.25 μm thickness was used for the separation of esters. Three minutes of equilibration time was set to raise the temperature to 150 °C, the isothermal temperature was maintained for 5 min and then raised to 250 °C at a rate of 7 °C/min, and the final temperature was maintained for 10 min. An ionization voltage of 70 eV over the scanning range of 450−750 amu was used to fragment the components. The components of the samples were identified by comparing the mass spectra with the National Institute of Standards And Technology Research Library (NIST-2014). Other operating conditions were injector temperature of 250 °C, interface temperature of 240 °C, and ion source temperature of 200 °C.

Further, nuclear magnetic resonance spectroscopy (NMR) (Bruker, 400 MHz) analyses were performed to analyze the fatty acid compositions of MCKO and MCKO-FAME and to determine the conversion (purity of produced fatty acid methyl esters) of MCKO to MCKO-FAME. The details of ^{1}H NMR analysis have been reported by several researchers.[2,44−46] A liquid sample of 40 μL was taken in a 5 mm NMR tube and mixed with 500 μL of deuterated chloroform ($CDCl_3$) solvent. The chemical shift peak of deuterated chloroform at 7.26 ppm was taken as the internal reference. The proton shift peaks of methyl ester and methylene were taken at around 3.65 and 2.31 ppm, respectively. The following equation (eq 7)[45] was used to determine the conversion (X) of MCKO to MCKO-FAME:

$$X(\%) = \frac{2 \times A_{\text{ME}}}{3 \times A_{\alpha\text{-CH}_2}} \times 100 \quad (7)$$

where X (%) is the percent conversion of MCKO triglycerides, A_{ME} is the integration value of the methyl ester proton peak area at around 3.65 ppm in the ^{1}H NMR profile, and $A_{\alpha\text{-CH2}}$ is the integration value of the carbonyl methylene proton peak area at around 2.31 ppm.

Engine Performance and Emission Characteristics. The *C. macrostachyus* oil fatty acid methyl esters obtained at optimum conditions were used for engine performance and emission characteristics analysis. Several FAMEs obtained from different feedstocks were tested with a blending ratio from 5 vol % (B5) to 20 vol % (B20) for engine performance and emission characteristics.[34,35,38,47,48] Hence, the blending ratios 5 (B5), 10 (B10), 15 (B15), and 20 vol % (B20) for *C. macrostachyus* kernel oil fatty acid methyl esters were used as they have not been reported before. For the present study, a four-stroke, single-cylinder, direct injection, and water-cooled diesel engine (R180 diesel engine) with a power output of 5.88 kW was used (Figure 1), and the details of the engine specification are presented in Table 2. The performance testing was done at a constant speed of 1500 rpm. The performance parameters of the diesel engine were measured in terms of the brake power (BP), brake thermal efficiency (BTE), brake

https://doi.org/10.1021/acsomega.2c00682
ACS Omega 2022, 7, 20619−20633

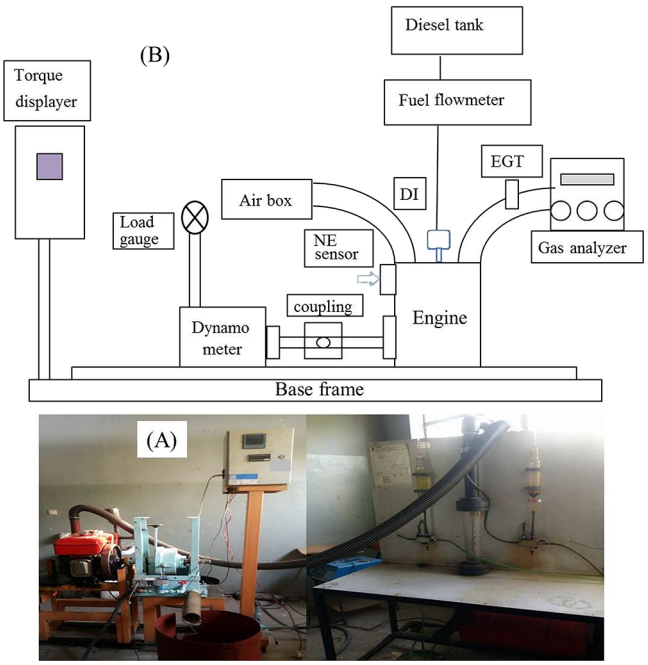

Figure 1. Experimental setup for the engine performance and emission test. (A) Photo image and (B) sketch.

Table 2. R180 Diesel Engine Specifications

engine type	four-cycle, single-cylinder horizontal R180 diesel engine
combustion system	precombustion chamber
bore × stroke (mm × mm)	80 × 80
net weight	70 kg
1 h output power	8 hp (5.88 kW)
rated speed (rpm)	2600
cooling system	evaporative
displacement (cc)	402
fuel consumption (g/hp·h)	≤278.8 g/kW·h
starting method	hand cranking (electric start)
lubrication system	splash lubricated by pressure injection

specific fuel consumption (BSFC), and exhaust gas temperature (EGT). The brake power, brake thermal efficiency, and brake specific fuel consumption were determined using eqs 8−12.[34] The concentrations of exhaust gaseous emissions such as unburned hydrocarbon (HC), carbon monoxide (CO), carbon dioxide (CO_2), and nitrogen oxides (NOx) were analyzed at the exhaust gas line using a digital gas analyzer (FGA 4100).

$$\mathrm{BP} = \frac{2\pi N\tau}{60,\,000} \tag{8}$$

$$\tau = 9.81 \times \omega \times R \tag{9}$$

$$M_f = \frac{\rho \times V}{t} \tag{10}$$

$$\mathrm{BSFC} = \frac{M_f}{\mathrm{BP}} \tag{11}$$

$$\mathrm{BTE} = \frac{\mathrm{BP}}{M_f \times \mathrm{CV}} \times 100 \tag{12}$$

where BP = brake power (kW), N = revolution per minute of the crank shaft, τ = torque applied due to the net load (Nm), ω = net load acting on the brake drum (kg), R = radius of the brake drum (m), M_f = mass flow rate of fuel consumed (kg/s), ρ = density of fuel (kg/m^3), V = volume of fuel (m^3), BSFC = brake specific fuel consumption, BTE = brake thermal efficiency (%), and CV = fuel heating value (kJ/kg).

Uncertainty Analysis. The selection of instrument condition, calibration, environment, observation, and test planning contribute to the experimental error and uncertainties.[48] Uncertainty analysis can be used to show that the experiments were accurate. The percentage uncertainties of the parameters for engine performance such as brake power output (BP), brake thermal efficiency (BTE), and brake specific fuel consumption (BSFC) were calculated using the percentage uncertainties of a burette and stopwatch for fuel flow measurement, density measurement, calorific value determination, and engine load measurement instruments. The errors for each measured parameters were recorded, and the accuracy of the instrument is listed in Table 3. The overall uncertainty

Table 3. Instrument Accuracy and Uncertainty

variables	accuracy	uncertainty (%)
engine load	±0.1 kg	±0.29
burette for fuel measurement	±2.0 cc	±2.10
speed measurement unit (rpm)	±1.0 rpm	±1.0
manometer (MM)	±1.0 rpm	±1.0
brake power (BP)	±0.26 kW	±0.33
brake specific fuel consumption (BSFC)	±0.05 g/kW·h	±0.18
brake thermal efficiency (BTE)	±0.32	±0.35
Gas analyzer		
carbon monoxide (CO)	±0.01 vol %	±0.24
carbon dioxide (CO_2)	±0.03%	±0.32
oxides of nitrogen (NOx)	±1.0 ppm	±1.13
unburned hydrocarbon (HC)	±1.0 ppm	±1.18

of the experiment was calculated using the principle of propagation of errors as shown in eq 13.[49] The overall uncertainty error values from the experiment and instrument errors are found to be less than 5% (3.10%), which signifies that the obtained experimental data are statistically significant.

$$\text{Uncertainty (\%)} = (\mathrm{BP}^2 + \mathrm{BTE}^2 + \mathrm{HC}^2 + {\mathrm{CO}_2}^2 + \mathrm{NOx}^2 + \mathrm{burette}^2 + \mathrm{mano}^2 + \mathrm{RPM}^2)^{1/2} \tag{13}$$

RESULTS AND DISCUSSION

Characterization of *C. macrostachyus* Kernel and Its Extracted Oil. About 60 wt % of the *C. macrostachyus* seed was kernel. The proximate analysis result shows that the moisture, ash, volatile matter, and fixed carbon content of the *C. macrostachyus* kernel were found to be 6.31, 4.5, 82, and 7.19 wt %, respectively. The obtained results were within the recommended range value for biodiesel production.[9] The average oil extracted from *C. macrostachyus* kernel was 52.50 ± 0.02 wt % using *n*-hexane for an extraction time of 5 h. The quality of oil can be expressed in terms of physico-chemical properties; for example, the acid value of the oil determines the process of transesterification. The acid value of CMKO was found to be less than 2.5 mg KOH/g; hence, direct degumming and transesterification were carried out to convert

https://doi.org/10.1021/acsomega.2c00682
ACS Omega 2022, 7, 20619−20633

Table 4. Comparison of Physico-chemical Properties of *C. macrostachyus* Kernel Oil with Other Nonedible Vegetable Oils

properties	CMKO[a]	CMSO[b]	RSO[c]	CO[d]	JO[e]	CMO[f]	test method
oil content (wt %)	52.5 ± 0.05%	53.34 ± 0.02	49.36	40−55	50−60	N/A[g]	N/A
density (g/cm^3)	0.886 ± 0.01	0.889 ± 0.1	0.910	0.9621	0.860−0.933	0.918	ASTM D4052
kinematic viscosity (mm^2/s)	44.22 ± 0.02	43.98 ± 0.08	13.13	231.22	37.0−54.8	64	ASTM D445
acid value (mg KOH/g)	4.545 ± 0.03	4.488 ± 0.41	24	7.05	0.92−6.16	3.34	ASTM D664
free fatty acid (FFA) (wt %)	2.273 ± 0.01	2.244 ± 0.18	12	3.5	0.18−3.40	1.68	ASTM D664
saponification value (mg KOH/g)	196.806 ± 0.03	195.89 ± 0.61	235.3	185.4	102.9−209	194.9	ISO 3657:2013

[a]*C. macrostachyus* kernel oil (present study). [b]*C. macrostachyus* seed oil.[9] [c]Rubber seed oil.[2] [d]Castor oil.[51] [e]Jatropha oil.[50] [f]*C. megalocarpus* oil.[52] [g]N/A: not applicable.

CMKO into CMKO-FAME. The density of the CMKO was similar to that of the previously studied *C. macrostachyus* seed oil (0.889 g/cm^3) and *Jatropha curcas* oil (0.860−0.933 g/cm^3)[50] and less than that of castor oil (0.9621 g/cm^3)[51] and rubber seed oil (0.910 g/cm^3) (Table 4). The kinematic viscosity of CMKO was found to be 44.22 ± 0.02 mm^2/s and within the range of *Jatropha curcas* oil kinematic viscosity (37.0−54.8 mm^2/s).[50] The result was far less than that of castor oil (231.22mm^2/s), which makes CMKO suitable for biodiesel production (Table 4).

Kernel Oil FAME Synthesis. As the transesterification reaction is a reversible reaction, an excess amount of reactant methanol was used. The results of the transesterification process of each run are presented in Table 5 along with the CMKO-FAME yield. The CMKO-FAME yield value indicates that there is an effect of the process parameters on the transesterification of CMKO. Thus, studying the parameter effect was vital to obtain the maximum yield with the optimum condition.

Table 5. RSM-CCD Experimental Matrix and Response for the CMKO-FAME Yield

process parameters			CMKO-FAME yield	
methanol to oil ratio (mol/mol)	catalyst loading (wt %)	reaction time (h)	actual yield (wt %)	predicted yield (wt %)
9.00	2.34	1.50	65	65.43
6.00	1.00	2.00	71	70.92
12.00	1.00	2.00	95	95.19
9.00	1.50	0.66	66	65.98
6.00	1.00	1.00	66	66.50
9.00	1.50	1.50	80.92	80.55
9.00	1.50	1.50	80.93	80.55
3.95	1.50	1.50	56	55.80
9.00	1.50	1.50	80.98	80.55
9.00	1.50	1.50	80	80.55
9.00	0.66	1.50	83	82.73
9.00	1.50	2.34	85	85.17
6.00	2.00	2.00	63	63.12
12.00	2.00	2.00	84	83.39
14.05	1.50	1.50	82	82.35
12.00	2.00	1.00	65	64.97
9.00	1.50	1.50	80.48	80.55
12.00	1.00	1.00	78	77.77
9.00	1.50	1.50	80	80.55
6.00	2.00	1.00	58	57.70

Model Fitting and Analysis of Variance (ANOVA). The response surface methodology comprising a central composite design with a three-level, three-factor design was used to investigate the interaction effect and optimize conditions for the transesterification of CMKO. Experimental parameters, ranges, and levels of independent variables investigated and results of the CCD design are shown in Table 5. Further, Table 5 shows also the experimental design and the actual and predicted biodiesel yields. The principal model analysis was based on the analysis of variance (ANOVA) that provides numerical information for the p value. The quadratic model was developed in terms of actual factors for the designed responses (eq 14). The models were found to be significant as the p values were much less than 0.05.

The stability of the model was validated using analysis of variance (ANOVA). From the predefined model, a quadratic model was suggested by RSM-CCD, and the model was further analyzed using ANOVA (Table 6). The output showed that the model was significant with p values less than 0.0001. The reference limit for p value was chosen as 0.05. The model F value of 976.55 indicates that the model is significant. There is only a 0.01% chance that an F value this large could occur maybe due to noise.[26,28,30,34] The regression coefficient (R^2) quantitatively explains the correlation between the experimental values and the predicted value for the yield of biodiesel. The value of R^2 is equal to 0.9989, which is close to 1.00, indicating the best fit of the model (Figure 2A). Hence, about 99.89% of the experimental results of transesterification reactions were explained by the model (eq 14), and only 0.11% of the total variance was not explained by the suggested regression model. Similarly, the adjusted determination coefficients (adj. R^2 and predicted R^2) have values of 0.9978 and 0.9942, respectively. These imply that the developed regression model was satisfactory for explaining the significance of the model. The ANOVA analysis in Table 6 shows that the linear terms A, B, and C; the quadratic terms A^2, B^2,

Table 6. Analysis of Variance (ANOVA) for the Transesterification of CMKO for the Response Function of the Yield of CMKO-FAME

source	DF	mean squares	F value	pro>F	remark
model	9	228.74	976.55	<0.0001	significant
A	1	849.75	3627.77	<0.0001	significant
B	1	361.58	1543.67	<0.0001	significant
C	1	444.97	1899.69	<0.0001	significant
AB	1	8.00	34.15	0.0002	significant
AC	1	84.50	360.75	<0.0001	significant
BC	1	0.50	2.13	0.1747	slightly significant
A^2	1	236.88	1011.29	<0.0001	significant
B^2	1	75.48	322.26	<0.0001	significant
C^2	1	44.54	190.16	<0.0001	significant
residuals	10	0.23			
lack of fit	5	0.25	1.18	0.4313	not significant

https://doi.org/10.1021/acsomega.2c00682
ACS Omega 2022, 7, 20619−20633

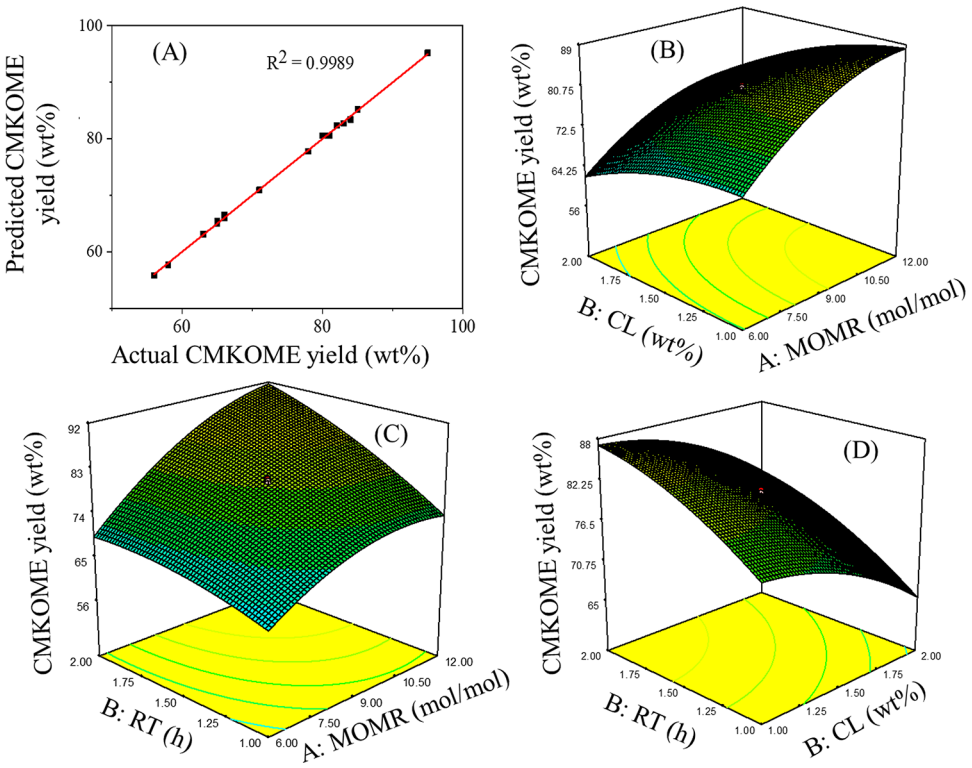

Figure 2. (A) Plot of actual vs predicted CMKO-FAME yield, (B) 3-D surface plot of methanol to oil ratio vs catalyst loading and reaction time, (C) 3-D surface plot of methanol to oil ratio vs reaction time, and (D) 3-D surface plot of catalyst loading vs reaction time.

and C^2; and the interaction term AC are significant model terms with p values less than 0.0001. Similarly, the linear interaction term AB was also a significant model term with a p value of 0.0002. However, the linear interaction term BC was a statistically not significant model term as the p value was greater than 0.05.

$$Y_{CMKOME} = 4.78993 + 8.47442A + 21.71411B + 11.5533C - 0.6667AB + 2.1667AC + 1.0BC - 0.4498A^2 - 9.1699B^2 - 7.0440C^2 \quad (14)$$

where Y_{CMKOME}: CMKO-FAME yield (wt %), A: methanol to oil molar ratio, B: catalyst loading (wt %), and C: reaction time (h).

Effect of Process Variables on FAME Yield. Important parameters that affect the transesterification of vegetable oil such as the molar ratio, catalyst loading, and reaction time were considered in the present study.[53] The 3-D curves of the response for the interactive as well as individual effects of independent variables are shown in Figure 2B–D. The effects of the methanol to oil molar ratio and catalyst loading on the CMKO-FAME yield while keeping the reaction time constant are shown in Figure 2B. As the reaction between reactant methanol and triglycerides of CMKO is reversible in nature, the molar ratio and catalyst loading are important to increase the reaction rate.[26,34,54] The two-dimensional (2-D) plots were also employed to explain the interaction between the other two variables. Based on the analysis of variance (ANOVA), the transesterification reaction was significantly affected by various interactions between the process variables (Table 6). Further, Figure 2B–D and the ANOVA result show that the significant individual process variables that affect the transesterification reaction are the methanol to oil molar ratio (A), catalyst concentration (B), and reaction time (C). As the reactant methanol and triglycerides of CMKO are immiscible in nature, the reaction time is important to increase the reaction rate.[55]

Interaction Effect between Process Variables on FAME Yield. From Figure 2B–D, it can be observed that the process variables have significant interaction effects on CMKO-FAME yield. The effect of both the process variables (reaction time and molar ratio) had a positive effect on the CMKO-FAME yield up to the optimal point, after which a further increase in the methanol or catalyst concentration did not increase the CMKO-FAME yield but rather caused a marginal decrease in the CMKO-FAME yield, resulting in the formation of soap and an increase in the cost of the postreaction steps.[28,54] The surface and contour plots show the relationships between the variables during their interaction. Each contour curve presents the effect of two variables on the CMKO-FAME yield, holding the third variable at a constant level. Figure 2B shows the 2-D contour and 3-D surface plot for the interaction effect of methanol to oil molar ratio versus catalyst concentration toward the CMKO-FAME yield. It can be noticed that the yield of CMKO-FAME increases with an increase in catalyst concentration toward 1.03 wt % up to 11.98:1 methanol to oil ratio and, after that, there is no substantial increase in the yield of biodiesel with an increase in the amount of methanol and catalyst concentration. A further increase in the catalyst loading dose resulted in a decrease in yield due to the formation of soap.[26,34] The contour plot revealed that more than 95% of CMKO-FAME yield was obtained at 11.98:1 methanol to oil ratio and 1.03 wt % catalyst concentration at 2 h reaction time. However, there is a reduction in the yield at higher methanol concentrations and catalyst concentrations. This is due to an increase in the solubility of glycerol leading to difficulties in the separation of

https://doi.org/10.1021/acsomega.2c00682
ACS Omega 2022, 7, 20619−20633

the ester layer as well as enhancing the backward transesterification reaction.[26,28,45]

Figure 2C shows the 2-D contour and 3-D surface plot for the interaction effect of methanol to oil ratio and reaction time. It was observed that at any of the methanol to oil molar ratios within the range, the yield increased with the increase in reaction time. Similarly, it was also observed that an increase in reaction time increased the CMKO-FAME yield.[56] At higher alcohol molar ratios and longer reaction times, a slight reduction in the yield could be observed due to the increase in the solubility of glycerol, which also favors the backward reaction to the left. Contour plots showed that the CMKO biodiesel yield of more than 90% was obtained between the intermediate to high reaction times and alcohol molar ratios.

Figure 2D shows the 2-D contour and 3-D surface plot for the interaction effect of reaction time and catalyst concentration on the CMKO-FAME yield. The result shows that at a low level of catalyst concentration, the yield increased with the increase of the time. However, at higher catalyst concentrations, the yield was less. This result was attributed to the fact that soap could be quickly formed, which made the separation of glycerol from biodiesel more difficult, thus reducing the yield.[14,16]

Optimization of Transesterification Process Parameters. The results obtained from RSM showed the three transesterification process variables and the interaction among the variables that affect the yield of CMKO-FAME. Therefore, the process variables were optimized using numerical optimization (Table 7). The model constraint was set for the methanol to oil molar ratio (6:1 to 12:1 molar ratio), reaction time (1 to 2 h), and catalyst loading (1 to 2 wt %). An optimum CMKO-FAME yield of 95.03 wt % was predicted at 11.98:1 methanol to oil molar ratio, 1.03 wt % catalyst concentration, and 2 h of reaction time. The model-predicted optimum value was experimentally validated by doing triplicate transesterification reaction experiments at optimum conditions, and it was found that 95.39 wt % of CMKO-FAME yield was experimentally obtained, which agreed well with the predicted value (95.03 wt %). Therefore, the model was useful to predict the yield of CMKO transesterification reaction using the KOH catalyst and also to obtain optimum process parameters for the transesterification reaction of CMKO. A similar observation was obtained from the ANOVA.

Table 7. Numerical Optimization Using RSM-CCD and Experimental Validation for Optimum Condition[a]

		level		
process parameters	goal	lower	upper	importance
methanol to oil ratio (mol/mol)	is in range	6	12	3
catalyst load (wt %)	is in range	1	2	3
reaction time (h)	is in range	1	2	3
CMOME (wt %)	maximize	56	95	5
Optimum condition for *C. macrostachyus* kernel oil fatty acid methyl ester yield				
process parameters	MOMR	CL	RT	*Y*
model-predicted value	11.98	1.03	2.0	95.03
experimental value	11.98	1.03	2.0	95.39
NMR results	11.98	1.03	2.0	95.52

[a]MOMR: methanol to oil molar ratio, CL: catalyst loading (wt %), RT: reaction time (h), and *Y*: CMKO-FAME yield (wt %).

Physico-chemical Properties of *Croton* Oil and Biodiesel. The important criterion of biodiesel quality is the inclusion of its physico-chemical properties presented in Tables 4 and 8. The current standards for regulating the quality of biodiesel on the market are varying based on a variety of factors. The quality standards for biodiesel fuel are continuously updated due to the evolution of ignition engines, ever-stricter emission standards, reevaluation of the eligibility of feedstocks used for the production of biodiesel, etc. The fatty acid methyl ester (biodiesel) produced from CMKO obtained at optimal conditions of 11.98:1 methanol to oil ratio, 1.03 wt % catalyst loading, 2 h reaction time, and 400 rpm agitation speed for reaction temperature of 60 °C was analyzed for fuel properties such as density, specific gravity, kinematic viscosity, moisture content, acid value, iodine value, ash content, saponification value, and flash points (Table 8). Some other properties like heating value and cetane number were estimated using empirical eqs 5 and 6 (Table 8). The viscosity of the oil increases with the increase in the molecular weight and decreases with the increase in the unsaturation level and temperature. A significant reduction in the kinematic viscosities of the samples was found from 44.22 (CMKO) to 4.58 mm^2/s (CMKO-FAME) during the transesterification. The value obtained for CMKO was much higher compared to conventional diesel; however, for CMKO-FAME, it is within the range of ASTM biodiesel standards and comparable with diesel fuel (Table 8). The obtained kinematic viscosity of CMKO-FAME (4.58 mm^2/s) was similar to that of CMSOME (4.6 mm^2/s), JSOME (4.2 mm^2/s), and cotton seed oil FAME (4.11 mm^2/s), whereas the value was less than that of NSOME (5.95 mm^2/s) (Table 8). The calorific value of the CMKO-FAME was estimated using eq 5 and found to be 40.017 MJ/kg. The value was higher than the JSOME caloric value (37.2

Table 8. Comparison of *C. macrostachyus* Oil Fatty Acid Methyl Ester with Other FAME and Petroleum Diesel Standards

						ASTM standard	
properties	CMKO-FAME[a]	CMSOME[b]	JSOME[c]	CSOME[d]	NSOME[e]	biodiesel	diesel
density (g/cm^3)	0.872	0.854	0.95	0.877	0.875	0.86–0.9	0.846
k. viscosity (mm^2/s)	4.58	4.6	4.2	4.11	5.95	1.9–6	1.9–4.1
acid value (mg KOH/g)	0.462	0.86	N/A[f]	0.19	0.81	0.5 max	N/A
free fatty acid (mg KOH/g)	0.231	0.43	N/A	0.095	0.41		N/A
calorific value (MJ/kg)	40.017	39.89	37.2	40.43	39.20	35 min	45.6–46.48
flash point (°C)	218	220	162	153	70	130 min	52–96
iodine value (mg I_2/g)	107.61	107.08	N/A	125.28	N/A	120 min	N/A
cetane number	50.78	N/A	53	55	53	47 min	40 min

[a]*C. macrostachyus* kernel oil fatty acid methyl ester (present study). [b]*C. macrostachyus* seed oil methyl ester.[9] [c]*Jatropha* seed oil FAME.[57] [d]Cottonseed oil FAME.[29] [e]Neem seed oil FAME.[58] [f]N/A: not applicable.

https://doi.org/10.1021/acsomega.2c00682
ACS Omega 2022, 7, 20619−20633

MJ/kg) (Table 8). The flash point is an important property of fuel to measure the flammability of fuel, safe storage, and use in the transportation sector. The flash point of the produced CMKO-FAME (218 °C) was higher than that of diesel fuel (52−96 °C), which shows that biodiesel is safer for storage. Moreover, the physico-chemical properties of CMKO-FAME were in agreement with the specifications of biodiesel under ASTM. The physico-chemical properties of MMKO-FAME such as kinematic viscosity, flash point, and density were reduced upon blending of diesel fuel (B0) for all blending ratios (B5, B10, B15, and B20), whereas the calorific value was increased (Table S1).

Fourier Transform Infrared (FT-IR) Spectroscopy Analysis. FT-IR spectroscopy has been considered as an experimental technique for the analysis of whether intensities of the bands in the spectrum are proportional to the concentration.[59] The FT-IR spectra in the mid-infrared region have been used to identify the functional groups and the bands corresponding to numerous stretching and bending vibrations in the samples of oils and FAMEs. The position of the carbonyl group in FT-IR is sensitive to substituent effects and to the structure of the molecule.[60] Basically, the esters have two characteristically strong absorption bands arising from carbonyl (−C═O) around 1750−1730 cm^{-1} and from −C−O (antisymmetric axial stretching and asymmetric axial stretching) at 1300−1730 cm^{-1}.[61] The stretching vibrations of $-CH_3$, $-CH_2$, and −CH appeared at 2980−2950, 2950−2850, and 3050−300 cm^{-1}, whereas the bending vibrations ($-CH_2$) of these groups appeared at 1475−1350, 1350−1150, and 709 cm^{-1}, respectively.[62] The spectrum of CMK, CMKO, and CMKO-FAME showed a triacylglycerol transmission band at 1743 cm^{-1}. The FT-IR spectra of CMKO and CMKO-FAME were almost similar, but various differences could be observed for the identification of the conversion of the CMKO into CMKO-FAME. The IR transmission peak shifting of the CMKO sample at 1748, 1377, 1157, 1026, and 856 cm^{-1} to 1742, 1361, 1168, 1015, and 878 cm^{-1} in the CMKO-FAME, respectively, were observed in the FT-IR spectra. The disappearance of peaks at 1450, 1157, and 709 cm^{-1} from the spectra of CMKO and appearance of new bands in CMKO-FAME at 1449 and 1172 cm^{-1} indicate the conversion of CMKO into CMKO-FAME. The spectra of CMK, CMKO, and CMKO-FAME showed a triacylglycerol absorption band at 1743 cm^{-1} (Figure 3).

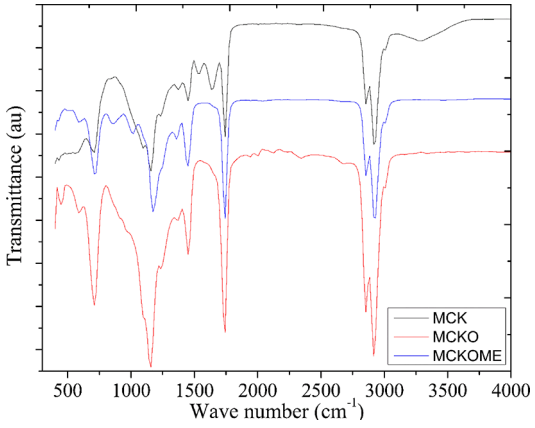

Figure 3. FT-IR spectra of *C. macrostachyus* kernel, its oil, and methyl esters.

Gas Chromatography−Mass Spectrometry (GC−MS) Analysis. Since the fatty acid composition influences the cetane number (CN) and cold flow properties of FAMEs, the determination of CMKO fatty acid composition was performed using GC−MS (Figure S1, supplementary results). The result shows that the CMKO contains fatty acid alkyl groups such as myristic acid (1.36%), palmatic acid (11.34%), stearic acid (5.11%), oleic acid (18.64%), linoleic acid (49.08%), linolenic acid (14.1%), and trace amount of gadoleic acid (0.34%) (Table 9). The GC−MS analysis shows that more than 50% of the fatty acid composition of the CMKO was unsaturated fatty acid alkyl groups.

Table 9. Fatty Acid Composition of *C. macrostachyus* Kernel Oil Fatty Acid Methyl Ester

peak no.	area (%)	systematic name	fatty acids	chemical structure
1	1.36	methyl tetradecanoate	myristic acid	C14:0
2	11.34	pentadecanoic acid, 14-methyl-, methyl ester	palmitic	C16:0
3	18.64	9-octadecenoic acid, methyl ester, (E)-	oleic acid	C18:1
4	49.08	9,11-octadecadienoic acid, methyl ester, (E,E)-	linoleic acid	C18:2
5	5.11	methyl stearate	stearic acid methyl ester	C18:0
6	14.1	9,12,15-octadecatrienoic acid, methyl ester, (Z,Z,Z)-	linolenic acid	C18:3
7	0.34	cis-11-eicosenoic acid, methyl ester	gadoleic acid	C20:1

Nuclear Magnetic Resonance (NMR) Spectroscopy Analysis. The CMKO and CMKO-FAME were characterized by ^1H NMR spectroscopy, and their spectra are shown in Figure S2A,B (supplementary results). The characteristic peak of methoxy protons was observed as a singlet at 3.65 ppm and a triplet of α-CH_2 protons at 2.27 ppm that were not present in the CMKO. This result shows that the triglyceride of CMKO is converted into its fatty acid methyl esters. Other observed peaks in both CMKO and CMKO-FAME were at 0.86 ppm of terminal methyl protons, a strong signal at 1.29 ppm related to methylene protons of the carbon chain, a signal at 1.59 ppm from β-carbonyl methylene protons, and a signal at 5.32 ppm due to olefinic hydrogen.[63] The ^1H NMR can also be used to calculate the conversion of vegetable oil to methyl esters via a transesterification reaction.[45] The relevant signals chosen for integration were those of the methoxy group in the methyl esters at 3.65 ppm and of the α-carbonyl methylene protons at 2.27 ppm[64] (Figure S2B). The percentage conversion of triglycerides in *C. macrostachyus* kernel oil to their corresponding methyl esters by using eq 7 was found to be 95.52%, which was quite in good agreement with the experimental yield of 95.39 wt % obtained as calculated by eq 1 and the model-predicted yield of 95.03 wt % obtained from the model equation (eq 14). The lower practical yield as compared to the calculated yield through the ^1H NMR study could be improved by giving more settling time to the product mixture or employing more efficient and appropriate separation processes. Further, the ^{13}C NMR (Figures S3−S4) shows that the spectra of both the samples were similar. However, from ^{13}C NMR (Figure S3), the peak observed at around 62 ppm for CH_2−C−O−and 68 ppm for CH−C−O− backbone signal triglyceride of CMKO in the CMKO sample is not present

https://doi.org/10.1021/acsomega.2c00682
ACS Omega 2022, 7, 20619−20633

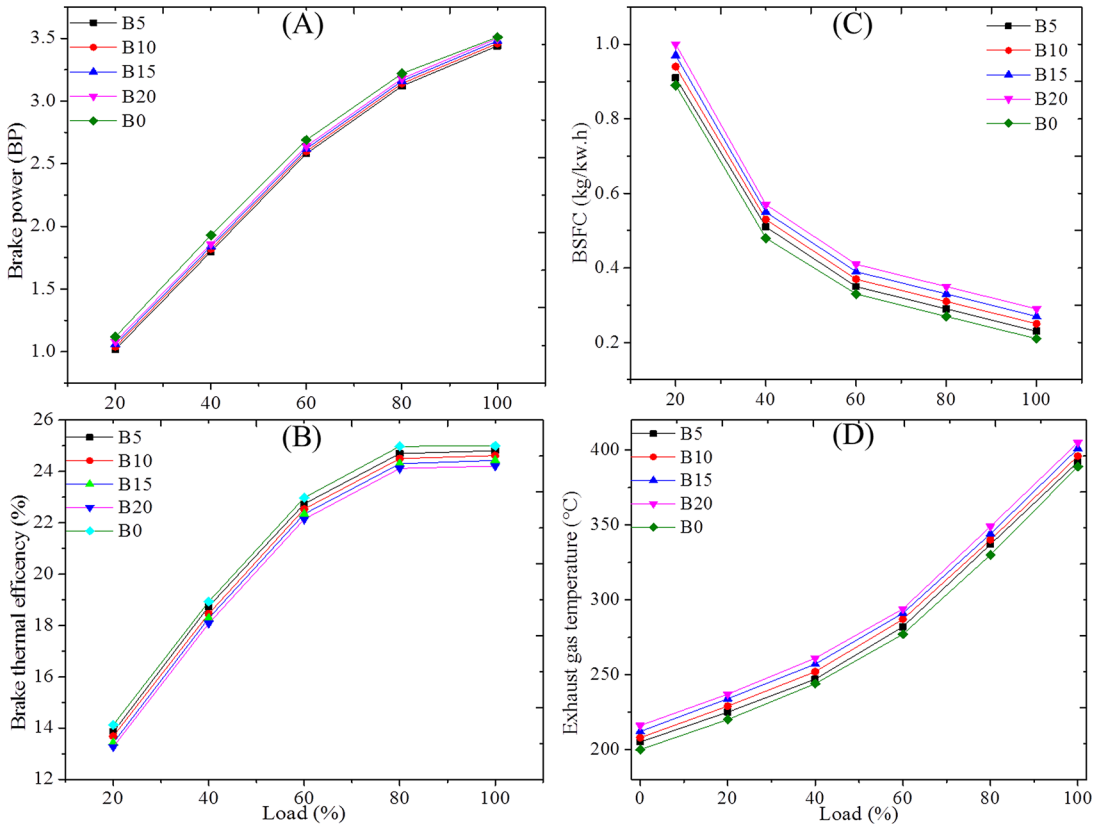

Figure 4. Effect of CMKO-FAME on engine performance: (A) brake power, (B) brake thermal efficiency, (C) brake specific fuel consumption, and (D) exhaust gas temperature.

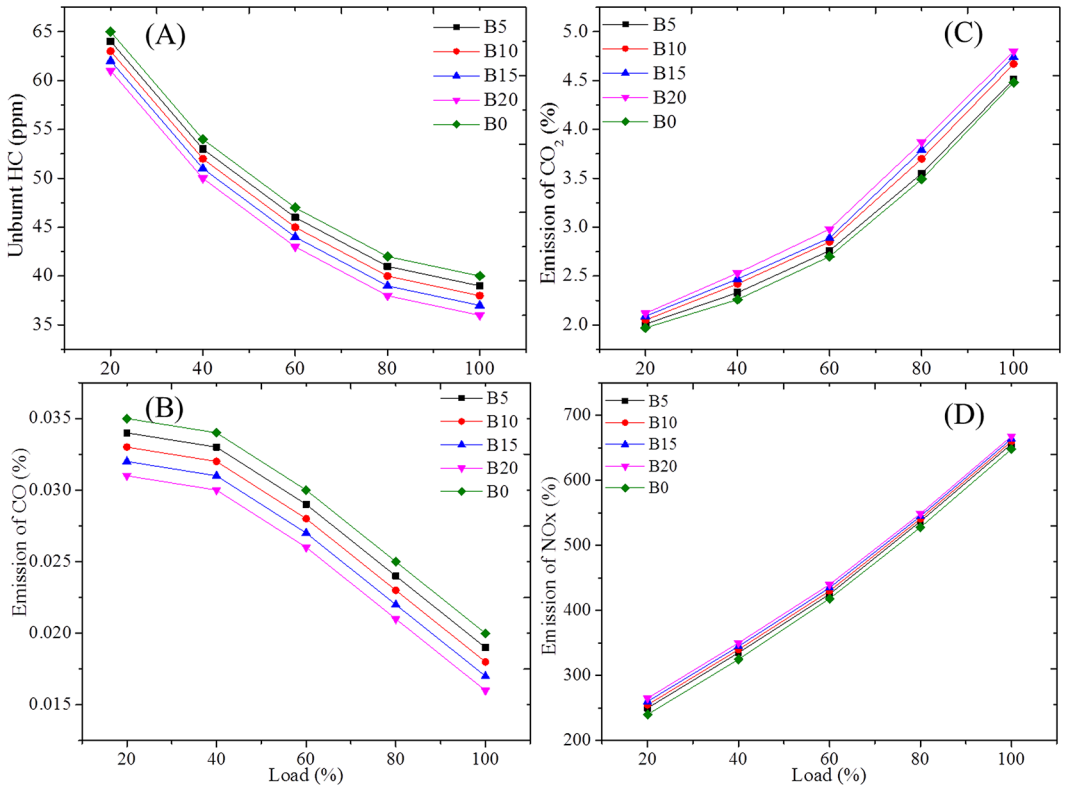

Figure 5. Effect of CMKO-FAME on emission characteristics of the engine: (A) unburnt HC emission, (B) incomplete combustion gas (CO) emission, (C) complete combustion gas (CO_2) emission, and (D) NOx emission.

https://doi.org/10.1021/acsomega.2c00682
ACS Omega 2022, 7, 20619−20633

in CMKO-FAME (Figure S4). The peaks at around 51 ppm appeared to further confirm the conversion of CMKO triglycerides into methyl esters of CMKO (Figure S4). The peaks around 131 and 127 ppm indicated the unsaturation in CMKO and its methyl esters (Figures S3 and S4). Other peaks at 14 ppm are due to the terminal carbon of methyl groups, and signals at 21−34 ppm are related to methylene carbons of the long carbon chain in the fatty acid methyl ester.

Engine Performance and Emission Characteristics Using Blends of Mineral Diesel Fuel and Produced CMKO-FAME. *C. macrostachyus kernel oil methyl ester blend properties.* The proper operation of an engine depends on a number of fuel properties and the results are presented in Table S1. The diesel engine performance and emissions of the diesel engine fueled with CMKO-FAME obtained at optimum conditions and petroleum diesel were investigated. The whole experiments were repeated three times, and the mean value was taken and presented in Figures 4A and D−5A−D, respectively. The results (Figure 5) show that biodiesel can be blended with diesel fuel in any proportion to improve the qualities of the fuel to reduce the emission (CO and HC).[65]

Engine Performance and Emission Characteristics. Engine performance tests were conducted for pure diesel without the CMKO-FAME blend (B0) and CMKO-FAME and diesel blends for B5, B10, B15, and B20 at various loads of engine (20−100% load) at 1500 rpm (Figure 4A−D). Brake power (BP) is the power measured at the crankshaft.[66] The brake power linearly increased when engine load increased from 20 to 100% at a constant speed of 1500 rpm. A similar trend was observed in the MCKO-FAME blended in diesel fuel (Figure 4A). However, in all engine loads, the brake powers were slightly reduced in all MCKO-FAME blends. This result may be due to the low calorific value of MCKO-FAME compared to the mineral diesel used.

Brake thermal efficiency (BTE) is the ratio of brake power output to the energy of fuel consumed, which is the product of the flow rate of injected fuel mass and the lower heating value.[66] On the other hand, it tells us the conversion of chemical energy of a fuel into mechanical energy. The BTE trends for mineral diesel fuel and its blend with MCKO-FAME with associated to brake power are shown in Figure 4B. As can be seen from Figure 4B, the BTE was found to be increased with the increase in engine load for diesel as well as for all tested blended CMKO-FAMEs. It was due to the higher load developing the power.[30,48] It is observed that BTE initially increases with the increase in load till 80% engine load; thereafter, a small change on BTE was observed for all cases, which was the maximum BTE. This was reasonable; with the further increase in load, heat losses also increase, leading to a decreasing value of BTE. The BTE (Figure 4B) for the blended fuel slightly decreased for all blending ratios at a fixed engine load due to its lower calorific value and high density of MCKO-FAME.[30,67] The maximum BTE in terms of percentage of diesel fuel is 25.0%, and those of CMKO-FAME blends B5, B10, B15, and B20 are 24.81, 24.62, 24.43, and 24.21%, respectively. This was also because of the lower calorific value and higher viscosity of CMKO-FAME that lead to the decreased atomization and mixing inside the combustion chamber and fuel vaporization resulting in lower values of BTE of the CMKO-FAME blend.[67] Based on the results, it can be concluded that the performance of the diesel engine with CMKO-FAME blends is comparable to that of mineral diesel fuel in terms of BTE.

Brake specific fuel consumption (BSFC) is a crucial criterion and measures the amount of burnt fuel to produce a given power. Figure 4C shows variations of BSFC when the engine was fueled with CMKO-FAME and diesel blend compared to mineral diesel fuel with respect to engine load. It was observed that BSFC was found to increase with an increase of CMKO-FAME concentrations in the fuel blends.[67] This is because a higher amount of CMKO-FAME is required to produce the same amount of energy as diesel due to the lower heating value and density of CMKO-FAME.[66,68] The highest value of BSFC was found for B20 due to the increased viscosity and lower calorific value of CMKO-FAME. At 100% load condition, the BSFC of B5, B10, B15, B20, and B0 (diesel) was found to be 0.23, 0.25, 0.27, 0.29, and 0.21 kg/kW h. Similarly, at 20% load condition, the BSFC of B5, B10, B15, B20, and B0 (pure diesel) was found to be 0.23, 0.25, 0.27, 0.29, and 0.21 kg/kW h. The maximum BSFC for mineral diesel fuel, B5, B10, B15, and B20 was observed at low loads of the engine, with a percentage variation of 2.25, 5.6, 8.99, and 12% for B5, B10, B15, and B20 as compared to diesel (B0). For the full load of the engine, the percentage differences for BSFC for all CMKO-FAME blend were increased to 9.8, 19.05, 28.6, and 38.1% for B5, B10, B15, and B20, respectively, as compared to diesel fuel (B0) for an engine load of 20%. The overall percentage difference increased for SFC for the blends as compared to diesel fuel (B0) was found to be 6.31, 12.4, 19.9, and 25.75% for B5, B10, B15, and B20, respectively. Similar findings were reported for castor oil methyl esters,[34] tallow biodiesel,[66] algae biodiesel,[69] *Salvinia molesta* oil biodiesel,[67] corn oil methyl esters,[70] and Mahua oil biodiesel.[71]

Exhaust gas temperature (EGT) is an indicator of the quality and efficiency for heat of fuels tested during the combustion process.[72,73] The EGTs of a diesel engine when fueled with pure diesel and its blend with CMKO-FAME (B5, B10, B15, and B20) at different engine loads are presented in Figure 4D. The result shows that the EGT values increased with the increase of the engine load for all the tested blend fuels (Figure 4D). The EGT of the diesel fuel was 330 °C, whereas for B5, B10, B15, and B20, the EGTs were 337, 340, 344, and 349 °C at 80% load. The higher EGT of about 216, 237, 261, 249, 349, and 405 °C was obtained at the minimum (0%) to full (100%) load when the engine was operated with B20. Overall, EGT rose when the concentration of CMKO-FAME increased in all engine loads due to the oxygen molecules present in CMKO-FAME that improve the fuel properties as well as improve combustion.[72,74] Hence, the lowest EGT values were obtained for mineral diesel fuel (B0), and the highest EGT values were observed for CMKO-FAME blend fuels. The percentage difference in the increase of EGT for the blends as compared to diesel fuel (B0) was found to be 1.4, 3.3, 5.27, and 6.45% for B5, B10, B15, and B20, respectively. This result also confirms the higher combustion of the test fuel that results in a higher EGT.[72,75]

Emission Analysis for CMKO-FAME Blends. The exhaust gas chemical composition such as unburned hydrocarbon (HC), carbon dioxide (CO_2), carbon mono oxide (CO), and nitrogen oxides (NOx) released from diesel engines during the combustion of the test fuels is a basic parameter of pollutants. Hence, in the analysis of combustion, these exhaust gases are the most important factors governing the process of improving internal combustion engines. The exhaust gas emission for the test fuel at different blending ratios and engine loads is presented in Figure 5A−D.

https://doi.org/10.1021/acsomega.2c00682
ACS Omega 2022, 7, 20619−20633

Unburnt Hydrocarbon (HC) Emission. HC emissions in exhaust gas that is transported in the form of vapor are mainly formed due to the incomplete combustion of fuel and express the nonutilizable chemical energy of fuel.[72,73,75] The main reason of HC in combustion product gases is the inability to reach the ignition temperature or lack of oxygen. The HC emission variation of different blends of CMKO-FAME fuel is shown Figure 5A. The HC emissions that resulted from CMKO-FAME blends were quite lower than those of diesel fuel. This was due to the fact that the oxygen molecule present in biodiesel results in improved combustion.[55,70,73−75] It was clearly observed that the HC emission for CMKO-FAME blends decreases with the increase in engine load, but it is lower than that of pure diesel (Figure 5A). These results are in agreement with various reported researches in which the reduction of HC was attributed to the high oxygen content in biodiesel that leads to complete combustion.[34,35,67,74] The maximum concentrations of HC emission are 64 (B5), 63 (B10), 62 (B15), 61 (B20), and 65 ppm (B0), respectively, indicating that this value declines as the concentration of CMKOME increases. On average, the HC in the exhaust gas was found to decrease by 2.07, 4.2, 6.24, and 8.32% while using the CMKO-FAME blend with B5, B10, B15, and B20, respectively. Similar results were observed for Karanja seed oil,[48] *Vachellia nilotica* seed oil,[35] *Salvinia molesta* oil,[67] and *Jatropha*−algae oil mixture[30] biodiesel blend with mineral diesel fuel.

Carbon Monoxide (CO) Emission. Carbon monoxide (CO) emission is a product of incomplete combustion due to the improper mixing of fuel with air and insufficient quantity of air in the air−fuel mixture. It is a common fact that the fatty acid methyl esters are oxygenated fuels,[34,72] which supply more oxygen (basically from 10 to 12%) for the complete combustion of CMKO-FAME−diesel blends than diesel fuel alone. Some other factors affecting the CO emission are cetane number, carbon to hydrogen ratio, and the existence of oxygen in the molecular structure. More oxygen is available for combustion in the cylinder, and more carbon molecules will be oxidized compared to diesel. The CO concentration was found to increase predominantly for pure diesel (B0), which was quite higher than emissions collected from other blended biodiesel fuels (Figure 5D). The results showed that the CO emission decreases as the engine load increases for all the test fuels as shown in Figure 5B. All CMKO-FAME blended fuels showed reduced CO emissions compared to pure diesel for all load conditions due to the presence of oxygen in the CMKO-FAME that enhances complete combustion.[47] At the maximum load of 100%, CO emission with diesel was 0.020 vol % compared to 0.019 vol % for B5, 0.018 vol % for B10, 0.017 vol % for B15, and 0.016 vol % for B20.[67] This shows the consumption of oxygen present in the CMKO-FAME chain for the conversion of CO formed into CO_2. It was observed that the peak concentrations obtained at a lower engine load (10%) were 0.034 (B5), 0.033 (B10), 0.032 (B15), 0.031 (B20), and 0.035% (B0). This implies that a higher CO emission was observed for lower CMKO-FAME blends, while a higher CO emission was seen for higher CMKO-FAME concentrations due to the higher combustion temperature at higher engine loads. It was observed that CO emissions decreased in the CMKO-FAME−diesel fueled engine, and similar results were reported for waste anchovy fish biodiesel blend,[72] castor seed oil biodiesel,[34] and soapnut oil methyl ester blend.[74]

Carbon Dioxide (CO_2) Emission. Carbon dioxide (CO_2) present in the exhaust gas emissions is an indication of the complete combustion of carbon in the fuel.[72,73] As shown in Figure 5C, the CO_2 emission increases with increasing engine load. It was also observed that the lowest CO_2 emissions were for B0 due to the incomplete combustion of diesel fuel. At lower concentrations of CMKO-FAME blends, lower amounts of CO_2 were emitted as compared to pure diesel fuel. As the concentration of CMKO-FAME in the blends increased, the CO_2 emission also increased. This was due to the oxygenated nature of the blended CMKO-FAME fuel.[76] The maximum CO_2 emission of 4.8% was observed at full load when the engine was operated with the 20% CMKO-FAME blend.

Nitrogen Oxide (NOx) Emission. NOx is the most toxic pollutant from diesel engine, and it must be controlled in the combustion chamber itself. Higher combustion temperature, longer combustion duration and higher oxygen concentrations are responsible for the formation of NOx emission.[76] Figure 5D shows the variation of NOx emission of diesel engine fueled with CMKO-FAME blends and pure diesel with respect to the loads. From Figure 5D, it was observed that the emission of NOx increased with the increase in engine loads for all tested fuel blends. It was also observed that the emission of NOx was lower for pure diesel fuel than that of all tested fuel blends. The higher concentration of CMKO-FAME in the blends contributes to the increased emission of NOx. At the full load condition, the NOx emission was recorded as 656, 660, 664, 668, and 648 ppm for B5, B10, B15, and B0, respectively.

CONCLUSIONS

Fatty acid methyl esters (FAMEs) were synthesized from *C. macrostachyus (Bisana)* kernel oil using the NaOH catalyst, and the resulting conversion of the oil was confirmed by FT-IR, GC−MS, and NMR (^{1}H and ^{13}C) analysis. Seven fatty acid alkyl groups were identified in *C. macrostachyus* kernel oil fatty acid methyl ester (CMKO-FAME) ranging from C14 to C20 containing 82.36% unsaturated fatty acid and 17.81% saturated fatty acid. The optimum conversion of 95.52 wt % for CMKO into its methyl ester was at the optimum reaction conditions of 11.98:1 methanol to oil molar ratio, 1.03 wt % NaOH catalyst loading, and reaction time of 2 h. The obtained quadratic model can predict the CMKO transesterification reaction with less than 0.5% error. The model can be employed to predict the yield of CMKO-FAME for large-scale processes to save time and maximize the CNKO transesterification process at various conditions within the range studied. The methyl esters produced at optimum conditions have acceptable properties well comparable with petro-diesel. The current study also presents the engine performance and emission characteristics of a diesel engine fueled with CMKO-FAME-diesel blends of B5, B10, B15, and B20. The engine performance results showed that the brake power and brake thermal efficiency of diesel are higher at all loads, but the brake specific fuel consumption of the CMKO-FAME blends is higher than that of diesel fuel. The brake specific fuel consumption increased with the increase in the quantity of CMKO-FAME and diesel in the blends and is higher than that in diesel fuel. The emission tests results showed that HC and CO emissions were lower for CMKO-FAME blends due to their higher oxygen content, but the CO_2 and NOx emissions were higher than those of conventional diesel. EGT was found to increase both concentrations of CMKO-FAME in the fuel blends and engine

https://doi.org/10.1021/acsomega.2c00682
ACS Omega 2022, 7, 20619−20633

loads. The overall results of the current study revealed that the *C. macrostachyus* seed is a promising feedstock for biodiesel production and the produced biodiesel is suitable in the diesel engine within studied range of blends (5 to 20 vol %) without modification of the diesel engine. Further, the combustion analysis of the *C. macrostachyus* kernel oil fatty acid methyl ester blend with mineral diesel fuel has to be considered in future research. Based on the current study finding, increasing the CMKO-FAME content in the blended fuel to use in diesel engines and cost analysis for larger-scale production of CMKO-FAME (biodiesel) are recommended for future research.

■ ASSOCIATED CONTENT

Supporting Information

The Supporting Information is available free of charge at https://pubs.acs.org/doi/10.1021/acsomega.2c00682.

GC−MS for *C. macrostachyus* kernel oil fatty acid methyl ester; ^{1}H NMR and ^{13}C NMR for *C. macrostachyus* kernel oil and its fatty acid methyl ester spectra; and physico-chemical properties of *C. macrostachyus* kernel oil fatty acid methyl ester, B5, B10, B15, B20, and B0 (PDF)

■ AUTHOR INFORMATION

Corresponding Author

Ali Shemsedin Reshad − *Department of Chemical Engineering, College of Biological and Chemical Engineering and Center of Excellence for Sustainable Energy Research, Addis Ababa Science and Technology University, Addis Ababa 16417, Ethiopia;* orcid.org/0000-0003-3695-954X; Email: ali.shemsedin@aastu.edu.et

Author

Zekarias Zeleke Zamba − *Department of Chemical Engineering, College of Biological and Chemical Engineering, Addis Ababa Science and Technology University, Addis Ababa 16417, Ethiopia; Department of Chemical Engineering, Defence Engineering College, Defence University, Bishoftu 1041, Ethiopia*

Complete contact information is available at: https://pubs.acs.org/10.1021/acsomega.2c00682

Funding

This study was funded by Addis Ababa Science and Technology University as Master student thesis work.

Notes

The authors declare no competing financial interest.

■ ACKNOWLEDGMENTS

Authors would like to acknowledge the Chemical Engineering Department, Addis Ababa Science and Technology University and Defence Engineering College, Ethiopia, for providing the characterization instruments to conduct the sample analyses and for providing the DI engine facilities, respectively.

■ REFERENCES

(1) Gebrenariam, S. N.; Marchetti, J. M. Biodiesel production technologies: A review. *AIMS Energy* **2017**, *5*, 425−457.

(2) Reshad, A. S.; Tiwari, P.; Goud, V. V. Extraction of oil from rubber seeds for biodiesel application: Optimization of parameters. *Fuel* **2015**, *150*, 636−644.

(3) Silitonga, A. S.; Masjuki, H. H.; Ong, H. C.; Yusaf, T.; Kusumo, F.; Mahlia, T. M. I. Synthesis and optimization of *Hevea brasiliensis* and *Ricinus communis* as feedstock for biodiesel production: A comparative study. *Ind. Crops Prod.* **2016**, *85*, 274−286.

(4) Randers, J., *A global forcast for the next forty years*; Chelsea Green Publishing: Norwegian, 2012.

(5) Jin, B.; Zhu, M.; Fan, P.; Yu, L.-J. Comprehensive utilization of the mixture of oil sediments and soapstocks for producing FAME and phosphatides. *Fuel Process. Technol.* **2008**, *89*, 77−82.

(6) Thomas, V. M.; Choi, D. G.; Luo, D.; Okwo, A.; Wang, J. H. Relation of biofuel to bioelectricity and agriculture Food security, fuel security, and reducing greenhouse emissions. *Chem. Eng. Res. Des.* **2009**, *87*, 1140−1146.

(7) Parthiban, K. S.; Perumalsamy, M. Nano sized heterogeneous acid catalyst from *Ceiba pentandra* stalks for production of biodiesel using extracted oil from *Ceiba pentandra* seeds. *RSC Adv.* **2015**, *5*, 11180−11187.

(8) Kusumo, F.; Silitonga, A. S.; Masjuki, H. H.; Ong, H. C.; Siswantoro, J.; Mahlia, T. M. I. Optimization of transesterification process for *Ceiba pentandra* oil: A comparative study between kernel-based extreme learning machine and artificial neural networks. *Energy* **2017**, *134*, 24−34.

(9) Aga, W. S.; Fantaye, S. K.; Jabasingh, S. A. Biodiesel production from Ethiopian "Besana"- *Croton macrostachyus* seed: Characterization and optimization. *Renewable Energy* **2020**, *157*, 574−584.

(10) Vicente, G.; Martinez, M.; Aracil, J. Integrated biodiesel production: a comparison of different homogeneous catalysts systems. *Bioresour. Technol.* **2004**, *92*, 297−305.

(11) Pauline, J. M. N.; Sivaramakrishnan, R.; Pugazhendhi, A.; Anbarasan, T.; Achary, A. Transesterification kinetics of waste cooking oil and its diesel engine performance. *Fuel* **2021**, *285*, No. 119108.

(12) Deng, X.; Fang, Z.; Liu, Y. Ultrasonic transesterification of Jatropha curcas L. oil to biodiesel by a two-step process. *Energy Convers. Manage.* **2010**, *51*, 2802.

(13) Georgogianni, K. G.; Kontominas, M. G.; Pomonis, P. J.; Avlonitis, D.; Gergis, V. Conventional and in situ transesterification of sunflower seed oil for the production of biodiesel. *Fuel Process. Technol.* **2008**, *89*, 503−509.

(14) Mostafaei, B.; Ghobadian, B.; Barzegar, M.; Banakar, A. Optimization of ultrasonic reactor geometry for biodiesel production using response surface methodology. *J. Agric. Sci. Technol.* **2013**, *15*, 697−708.

(15) Savaliya, M. L.; Patel, J. R.; Dholakiya, B. Z. A concise review on acid, alkali and enzyme catalyzed transesterification of fatty acid esters of glycerol (FAEG) to fatty acid methyl ester (FAME) Fuel. *Int. J. Chem. Stud.* **2013**, *1*, 1−15.

(16) Asmare, M.; Gabbiye, N. Synthesis and characterization of biodiesel from castor bean as alternative fuel for diesel engine. *Am. J. Energy Eng.* **2014**, *2*, 1−15.

(17) Meher, L. C.; Dharmagadda, V. S. S.; Naik, S. N. Optimization of alkali-catalyzed transesterification of *Pongamia pinnata* oil for production of biodiesel. *Bioresour. Technol.* **2006**, *97*, 1392−1397.

(18) Arshad, M.; Zia, M. A.; Shah, F. A.; Ahmad, M. An overview of biofuel. In *Perspectives on water usage for biofuels production*, Arshad, M., Ed. Springer Nature, 2018; pp. 1−37.

(19) Lee, H. V.; Yunus, R.; Juan, J. C.; Taufiq-Yap, Y. H. Process optimization design for jatropha-based biodiesel production using response surface methodology. *Fuel Process. Technol.* **2011**, *92*, 2420−2428.

(20) bezerra, M. A.; Santelli, R. E.; Oliveira, E. P.; Villar, L. S.; Escalerira, L. A. Response surface methodology (RSM) as a tool for optimization in analytical chemistry. *Talanta* **2008**, *76*, 965−977.

(21) Gul, M.; Zulkifli, N. W. M.; Kalam, M. A.; Masjuki, H. H.; Mujtaba, M. A.; Yousuf, S.; Bashir, M. N.; Ahmed, W.; Yusoff, M. N. A. M.; Noor, S.; Ahmad, R.; Hassan, M. T. RSM and Artificial Neural Networking based production optimization of sustainable Cotton biolubricant and evaluation of its lubricity & tribological properties. *Energy Rep.* **2021**, *7*, 830−839.

(22) Onukwuli, D. O.; Esonye, C.; Uwaom, A.; Eyisi, O. R. Artificial neural network-genetic algorithm (ANN-GA) and response surface methodology (RSM) were used to predict the optimal process conditions for biodiesel synthesis. *J. Taiwan Inst. Chem. Eng.* **2021**, *125*, 153−167.
(23) Pilkington, J. L.; Preston, C.; Gomes, R. L. Comparison of response surface methodology (RSM) and artificial neural networks (ANN) towards efficient extraction of *artemisinin from Artemisia annua*. *Ind. Crops Prod.* **2014**, *58*, 15−24.
(24) Dantas, T. N. C.; Cabral, T. J. O.; Neto, D. A. A.; Moura, M. C. P. A. Enrichmnent of patchoulol extracted from patchouli (*Pogostemon cablin*) oil by molecular distillation using response surface and artificial neural network models. *J. Ind. Eng. Chem.* **2020**, *81*, 219.
(25) Esonye, C.; Onukwuli, O. D.; Ofoefule, A. U. Optimization of methyl ester production from *Prunus Amygdalus* seed oil using response surface methodology and Artificial Neural Networks. *Renewable Energy* **2019**, *130*, 61−72.
(26) Reshad, A. S.; Panjiara, D.; Tiwari, P.; Goud, V. V. Two-step process for production of methyl ester from rubber seed oil using barium hydroxide octahydrate catalyst: Process optimization. *J. Cleaner Prod.* **2017**, *142*, 3490.
(27) Shuit, S. H.; Lee, K. T.; Kamaruddin, A. H.; Yusup, S. Reactive extraction of *Jatropha curcas L* . seed for production of biodiesel process optimization study. *Environ. Sci. Technol.* **2010**, *44*, 4361−4367.
(28) Mekonnen, K. D.; Sendekie, Z. B. NaOH-catalyzed methanolysis optimization of biodiesel synthesis from desert date seed kernel oil. *ACS Omega* **2021**, *6*, 21082−24091.
(29) Mourshed, M.; Ghosh, S. K.; Islam, W. Experimental investigation of cotton (*Gossypium hirsutum*) seed oil and neem (*Azadirachta indica*) seed oil methyl esters as biodiesel on di (direct injection) engine. *Int. J. Ambient Energy* **2022**, 1772−1782.
(30) Kumar, S.; Jain, S.; Kumar, H. Experimental Study on Biodiesel Production Parameter optimization of Jatropha-algea oil mixtures and performance and emission analysis of a diesel engine coupled with a generatore fuled with diesel and bidiesel blendes. *ACS Omega* **2020**, *5*, 17033−17041.
(31) Borah, M. J.; Das, A.; Das, V.; Bhuyan, N.; Deka, D. Transesterification of waste cooking oil for biodiesel production catalyzed by Zn substituted waste egg shell derived CaO nanocatalyst. *Fuel* **2019**, *242*, 345−354.
(32) Yatish, K. V.; Lalithamba, H. S.; Suresh, R.; Hebbar, H. R. H. Optimization of bauhinia variegata biodiesel production and its performance, combustion and emission study on diesel engine. *Renewable Energy* **2018**, *122*, 561−575.
(33) Borah, M. J.; Devi, A.; Saikia, R. A.; Deka, D. Biodiesel production from waste cooking oil catalyzed by in-situ decorated TiO_2 on reduced graphene oxide nanocomposite. *Energy* **2019**, *158*, 881−889.
(34) Dasari, S. R.; Chaudhary, A. J.; Goud, V. V.; Sahoo, N.; Kulkarni, V. N. *In-situ* alkaline transesterification of castor seeds: Optimization and engine performance, combustion and emission characteristics of blends. *Energy Convers. Manage.* **2017**, *142*, 200−214.
(35) Sriharikota, C. S.; Karuppasamy, K.; Nagarajan, V.; Sathyamurthy, R.; Ramani, B.; Muthu, V.; Karuppiah, S. Experimental investigation of the emission and performance characteristics of a DI diesel engine fueled with the *Vachellia nilotica* seed oil methyl ester and diesel blends. *ACS Omega* **2021**, *6*, 14068−14077.
(36) Dhar, A.; Agarwal, A. K. Performance, emissions and combustion characteristics of Karanja biodiesel in a transportation engine. *Fuel* **2014**, *119*, 70−80.
(37) Raheman, H.; Ghadge, S. V. Performance of compression ignition engine with mahua (*Madhuca indica*) biodiesel. *Fuel* **2007**, *86*, 2568−2573.
(38) Khiari, K.; Awad, S.; Loubar, K.; Tarabet, L.; Mahmoud, R.; Tazerout, M. Experimental investigation of pistacia lentiscus biodiesel as a fuel for direct injection diesel engine. *Energy Convers. Manage.* **2016**, *108*, 392−399.
(39) Ong, H. C.; Masjuki, H. H.; Mahlia, T. M. I.; ASilitonga, A. S.; Chong, W. T.; Leong, K. Y. Optimization of biodiesel production and engine performance from high free fatty acid *Calophyllum inophyllum* oil in CI diesel engine. *Energy Convers. Manage.* **2014**, *81*, 30−40.
(40) Puhan, S.; Jegan, R.; Balasubbramanian, K.; Nagarajian, G. Effect of injection pressure on performance, emission and combustion characteristics of high linolenic linseed oil methyl ester in a DI diesel engine. *Renewable Energy* **2009**, *34*, 1227−1233.
(41) Utlu, Z.; Kocak, M. S. The effect of biodiesel fuel obtained from waste frying oil on direct injection diesel engine performance and exhaust emissions. *Renewable Energy* **2008**, *33*, 1936−1941.
(42) Ilham, Z.; Saka, S. Two-step supercritical dimethyl carbonate method for biodiesel production from *Jatropha curcas* oil. *Bioresour. Technol.* **2010**, *101*, 2735−2740.
(43) Demirbas, A. Relationships derived from physical properties of vegetable oil and biodiesel fuels. *Fuel* **2008**, *87*, 1143−1148.
(44) Das, S.; Thakur, A. J.; Deka, D. Two-stage conversion of high free fatty acid *Jatropha curcas* oil to biodiesel using brønsted acidic ionic liquid and KOH as catalysts. *Sci. World J.* **2014**, No. 180983.
(45) Farooq, M.; Ramli, A.; Subbarao, D. Biodiesel production from waste cooking oil using bifunctional heterogeneous solid catalysts. *J. Cleaner Prod.* **2013**, *59*, 131−140.
(46) Yeung, D. K. W.; Lam, S. L.; Griffith, J. F.; Chan, A. B. W.; Chen, Z.; Tsang, P. H.; Leung, P. C. Analysis of bone marrow fatty acid composition using high-resolution proton NMR spectroscopy. *Chem. Phys. Lipids* **2008**, *151*, 103−109.
(47) Kumar, M. V.; Babu, A. V.; Kumar, P. R. Experimental investigation on mahua methyl ester blended with diesel fuel in a compression ignition diesel engine. *Int. J. Ambient Energy* **2017**, 304−316.
(48) Sivaramakrishnan, K. Investigation on performance and emission characteristics of a variable compression multi fuel engine fuelled with Karanja biodiesel−diesel blend. *Egypt. J. Pet.* **2018**, *27*, 177−186.
(49) Mubarak, M. Performance, emission and combustion characteristics of low heat rejection diesel engine using waste cooking oil as fuel. *Int. J. Ambient Energy* **2022**, 303−313.
(50) Koh, M. Y.; Ghazi, T. I. M. A review of biodiesel production from *Jatropha curcas L. oil. Renewable Sustainable Energy Rev.* **2011**, 2240.
(51) Keera, S. T.; EI Sabagh, S. M.; Taman, A. R. Castor oil biodiesel production and optimization. *Egypt. J. Pet.* **2018**, *27*, 979−984.
(52) Kafuku, G.; Mbarawa, M. Biodiesel production from *Croton megalocarpus* oil and its process optimization. *Fuel* **2010**, *89*, 2556−2560.
(53) Onukwuli, D. O.; Emembolu, L. N.; Ude, C. N.; Aliozo, S. O.; Menkiti, M. C. Optimization of biodiesel production from refined cotton seed oil and its characterization. *Egypt. J. Pet.* **2017**, *26*, 103−110.
(54) Bello, E. I.; Ogedengbe, T. I.; Lajide, L.; Daniyan, I. A. Optimization of process parameters for biodiesel production using Response surface methodology. *Am. J. Energy Eng.* **2016**, *4*, 8−16.
(55) El-Gendy, N.; Deriase, S. F.; Hamdy, A.; Abdallah, R. I. Statistical optimization of biodiesel production from sunflower waste cooking oil using basic heterogeneous biocatalyst prepared from eggshells. *Egypt. J. Pet.* **2015**, *24*, 37−48.
(56) Abba, E. C.; Nwakuba, N. R.; Obasi, S. N.; Enem, J. I. Effect of reaction time on the yield of biodiesel from Neem seed oil. *Am. J. Energy Sci.* **2017**, *4*, 5−9.
(57) Kadry, G. A. Biodiesel production from Jatropha seeds. *Am. J. Chem. Eng.* **2015**, *3*, 89−98.
(58) Anwar, M. Biodiesel feedstocks selection strategies based on economic, technical, and sustainable aspects. *Fuel* **2021**, *283*, No. 119204.

https://doi.org/10.1021/acsomega.2c00682
ACS Omega 2022, 7, 20619−20633

(59) Guerrero-Perez, M. O.; Patience, G. S. Experimental methods in chemical engineering: Fourier transform infrared spectroscopy—FTIR. *Can. J. Chem. Eng.* **2020**, *98*, 25−33.
(60) Bianchi, G.; Howarth, O. W.; Samuel, C. J.; Vlahov, G. Long-range σ-inductive interactions through saturated C−C bonds in polymethylene chains. *J. Chem. Soc., Perkin Trans. 2* **1995**, *2*, 1427.
(61) Soares, I. P.; Rezende, T. F.; Silva, R. C.; Castro, E. V. R.; Fortes, I. C. P. Multivariate calibration by variable selection for blends of raw soybean oil/biodiesel from different sources using Fourier transform infrared spectroscopy (FTIR) spectra data. *Energy Fuels* **2008**, *22*, 2079−2083.
(62) McCuen, R. A guide to complete interperetation of infrared spectra of organic structures. *J. Am. Water Resour. Assoc.* **2010**, *46*, 1060−1064.
(63) Monteiro, M. R.; Ambrozin, A. R. P.; Liao, L. M.; Ferreira, A. G. Determination of biodiesel blend levels in different diesel samples by ^{1}H NMR. *Fuel* **2009**, *88*, 691−696.
(64) Naureen, R.; Tariq, M.; Yusoff, I.; Chowdhury, A. J. K.; Ashraf, M. A. Synthesis, spectroscopic and chromatographic studies of sunflower oil biodiesel using optimized base catalyzed methanolysis. *Saudi J. Biol. Sci.* **2015**, *22*, 332−339.
(65) Hasan, M. M.; Rahman, M. M. Performance and emission characteristics of biodiesel−diesel blend and environmental and economic impacts of biodiesel production: A review. *Renewable Sustainable Energy Rev.* **2017**, *74*, 938−948.
(66) Gautam, R.; Kumar, S. Performance and combustion analysis of diesel and tallow biodiesel in CI engine. *Energy Rep.* **2020**, *6*, 2785−2793.
(67) Mubarak, M.; Shaija, A.; Suchithra, T. V. Experimental evaluation of *Salvinia molesta* oil biodiesel/diesel blends fuel on combustion, performance and emission analysis of diesel engine. *Fuel* **2021**, *287*, No. 119526.
(68) Qasim, M.; Ansari, T. M.; Hussain, M. Combustion, performance, and emission evaluation of a diesel engine with biodiesel like fuel blends derived from a mixture of Pakistani waste canola and waste transformer oils. *Energies* **2017**, *10*, 1023.
(69) Elkelawy, M.; Bastawissi, H. A.-E.; El Shenawy, E. A.; Taha, M.; Pachal, H.; Sadasivuni, K. K. Study of performance, combustion, and emissions parameters of DI-diesel engine fueled with algae biodiesel/diesel/n-pentane blends. *Energy Convers. Manage.: X* **2021**, *10*, No. 100058.
(70) Sathyamurthy, R.; Balaji, D.; Gorjian, S.; Muthiya, S. J.; Bharathwaaj, R.; Vasanthaseelan, S.; Essa, F. A. Performance, combustion and emission characteristics of a DI-CI diesel engine fueled with corn oil methyl ester biodiesel blends. *Sustainable Energy Technol. Assess.* **2021**, *43*, No. 100981.
(71) Kannan, M.; Elavarasan, G.; Karthikeyan, D.; Goyat, V. Analysis of emission and performance characteristics of compression ignition engine using Mahua oil-based biodiesel. *Mater. Today: Proc.* **2021**, *46*, 10142−10146.
(72) Bechet, R. Performance and emission study of waste anchovy fish biodiesel in a diesel engine. *Fuel Process. Technol.* **2011**, *92*, 1187−1194.
(73) Elkelawy, M.; Bastawissi, H. A.-E.; Esmaeil, K. K.; Radwan, A. M.; Pachal, H.; Sadasivuni, K. K. Experimental studies on the biodiesel production parameters optimization of sunflower and soybean oil mixture and DI engine combustion, performance, and emission analysis fueled with diesel/biodiesel blends. *Fuel* **2019**, *255*, No. 115791.
(74) Venkatesan, V.; Nallusamy, N.; Nagapandiselvi, P. Performance and emission analysis on the effect of exhaust gas recirculation in a tractor diesel engine using pine oil and soapnut oil methyl ester. *Fuel* **2021**, *290*, No. 120077.
(75) Saleh, H. E. Performance and emissions characteristics of direct injection diesel engine fueled by diesel-jojoba oil-butanol blends with hydrogen peroxide. *Fuel* **2021**, *285*, No. 119048.
(76) Ogunkunle, O.; Ahmed, N. A. Exhaust emissions and engine performance analysis of a marine diesel engine fuelled with *Parinari polyandra* biodiesel−diesel blends. *Energy Rep.* **2020**, *9*, 2999−3007.

https://doi.org/10.1021/acsomega.2c00682
ACS Omega 2022, 7, 20619−20633